Free Radical Research, March 2010; 44(3): 249–257

Determination of reactive oxygen species associated with the degeneration of dopaminergic neurons during dopamine metabolism

MAYUMI YAMATO[1,2], WATARU KUDO[1], TAKESHI SHIBA[1,3], KEN-IICHI YAMADA[3], TOSHIAKI WATANABE[1] & HIDEO UTSUMI[3]

[1]Department of REDOX Medicinal Science, Faculty of Pharmaceutical Sciences, Kyushu University, Fukuoka, [2]Medical Redox Imaging Group, Innovation Center for Medical Redox Navigation, Kyushu University, Fukuoka, and [3]Department of Bio-function Science, Faculty of Pharmaceutical Sciences, Kyushu University, Fukuoka, Japan

(Received date: 8 July 2009; In revised from date: 30 September 2009)

Abstract

Oxidative stress is believed to be an important mechanism underlying dopamine-induced neuronal damage. This study provides X-band electron spin resonance (ESR) spectroscopic evidence for reactive oxygen species (ROS) generation during dopamine metabolism. The authors induced excess dopamine metabolism in the mouse striatum by bathing it in tyramine-containing perfusate using microdialysis. The addition of tyramine to the perfusate raised the levels of extracellular dopamine and hydrogen peroxide significantly. The ESR signal from hydroxy-TEMPO decayed during tyramine perfusion and treatment with a monoamine-oxidase inhibitor or radical scavenger suppressed the signal decay. Decreases in the number of tyrosine hydroxylase-immunopositive fibres and in dopamine concentration after tyramine perfusion were observed. Moreover, the tyramine-perfused mice showed a marked methamphetamine-induced rotational response. Notably, these effects of tyramine were suppressed by the simultaneous perfusion of hydroxy-TEMPO. These findings indicate that the ROS generation, which was monitored by hydroxy-TEMPO, caused oxidative damage to the dopaminergic neurons.

Keywords: *Oxidative stress, reactive oxygen species, free radical, Tempol, nitroxide, dopamine.*

Introduction

Dopamine plays an important role in modulating voluntary movements in the brain and alterations in dopaminergic function are closely linked to the pathology of motor/movement disorders such as Parkinson's disease. Although dopamine has a physiological role as an essential neurotransmitter, it can also act as a toxic agent and vulnerability factor for neurodegeneration [1,2]. For example, the high extracellular dopamine in dopamine transporter-knockout mice is neurotoxic to presynaptic dopaminergic neurons [3]. In addition, the rate-controlling enzyme of dopamine biosynthesis, tyrosine hydroxylase (TH), is significantly decreased by an intrastriatal injection of a high dose of dopamine [4].

Oxidative stress is thought to play a major role in dopamine-induced neuronal damage. A small fraction of dopamine is taken up into the cytosol and is metabolized at the mitochondrial outer membrane, which leads to its neurotoxic effects. Transgenic mice in which striatal neurons were engineered to take up extracellular dopamine developed motor dysfunctions and progressive neurodegeneration in the striatum via dopamine metabolism and oxidation [5]. Cytosolic dopamine undergoes degradation to form 3,4-dihydroxyphenylacetic acid (DOPAC) and homovanillic acid (HVA) as well as hydrogen peroxide (H_2O_2) via the monoamine oxidase (MAO) pathway [6]. Mallajosyula et al. [7] demonstrated that an elevation in the astrocytic monoamine oxidase-B (MAO-B) level resulted in increased H_2O_2 and a relatively selective loss of dopaminergic neurons. Moreover, the cytotoxic hydroxyl radical (•OH), which is generated by interactions between H_2O_2 and

Correspondence: Mayumi Yamato, Medical Redox Imaging Group, Innovation Center for Medical Redox Navigation, Kyushu University, Fukuoka 812-8582, Japan. Tel: +81-92-642-6031. Fax: +81-92-642-6024. Email: yamato68@redoxnavi.med.kyushu-u.ac.jp

ISSN 1071-5762 print/ISSN 1029-2470 online
DOI: 10.3109/10715760903456084

transition metals in the brain, may damage dopaminergic neurons [8]. However, despite much conjecture about the nature of the oxidative stress caused by dopamine metabolism, there is little experimental evidence for the direct elevation of a factor responsible for the degeneration.

The methods for detecting reactive oxygen species (ROS) such as •OH in biological systems involve the introduction of a spin-trapping agent that competes with the cellular molecules and electron spin resonance (ESR, also known as electron paramagnetic resonance, EPR) spectroscopy is a convenient method for their detection [9], because ROS are highly reactive and short-lived species. Although spin-trapping is used for the direct analysis of radical intermediates, its sensitivity may be limited by the low stability of the spin adducts *in vivo*.

Nitroxyl radicals have been used as antioxidants to protect animal tissues from oxidative damage [10,11]. The effective reactions of nitroxyl radicals with ROS such as superoxide anion radical and •OH are generally proved to be a key mechanism for antioxidant function. Willson [12] suggested that the final product might be the oxoammonium cation, when •OH reacts with the nitroxyl group of 4-hydroxy-2,2,6,6-tetramethylpiperidine-N-oxyl (hydroxy-TEMPO, i.e. Tempol) at almost the diffusion-controlled rate [13]. The oxoammonium cation was reduced to the hydroxylamine by NADH [14]. In addition, we successfully detected the generation of ROS by dopamine metabolism *in vitro* using hydroxy-TEMPO as a spin probe for ESR spectroscopy [15]. We also showed that the reaction between hydroxy-TEMPO and ROS converted the nitroxyl radical form of the probe to its corresponding hydroxylamine form in the presence of NADH. The effective reaction of hydroxy-TEMPO with ROS during dopamine metabolism may be proved to be a key mechanism for antioxidant function. Therefore, in this study, we used the ESR/spin probe technique to provide direct evidence of ROS generation during dopamine metabolism *in vivo*, by stimulating its metabolism with tyramine, an endogenous trace amine that is known to increase the extracellular dopamine level [16]. Furthermore, we found that the generation of ROS was correlated with decreased TH immunoreactivity and methamphetamine-induced rotational behaviour.

Materials and methods

Chemicals

4-Hydroxy-2,2,6,6-tetramethylpiperidine-1-oxyl (hydroxy-TEMPO), 4-carboxy-2,2,6,6-tetramethylpiperidine-1-oxyl (carboxy-TEMPO), deferoxamine mesylate salt, tyramine hydrochloride, 3-methoxytyramine hydrochloride (3-MT), 1,3-dimethyl-2-thiourea (DMTU), tranylcypromine hydrochloride, pargyline hydrochloride and alpha-methyl-p-tyrosine were purchased from Sigma-Aldrich Co. (St. Louis, MO). Sodium dihydrogenphosphate dehydrate, citric acid, trichloroacetic acid, sodium L-ascorbate, ferrous sulphate dihydrate, sodium acetate trihydrate, potassium hexacyanoferrate, ethylenediamine-N,N,N',N'-tetraacetic acid disodium salt, 1-heptanesulphonic acid sodium salt, hydrogen peroxide, calcium chloride, potassium chloride, magnesium chloride, phosphoric acid, perchloric acid, zinc sulphate heptahydrate, horseradish peroxidase, dopamine, 3,4-dihydroxyphenylacetic acid (DOPAC), homovanillic acid (HVA), catalase (from bovine liver) and lithium perchlorate were purchased from Wako Pure Chemical Industries (Osaka, Japan). Isoflurane and pentobarbital were purchased from Dainihon Pharmaceutical Co. (Osaka, Japan). Methanol and acetonitrile (HPLC grade) were purchased from Nacalai Tesque, Inc. (Kyoto, Japan).

HPLC standards were dissolved in perchloric acid (100 mmol/L). Tranylcypromine, pargyline and alpha-methyl-*p*-tyrosine were dissolved in saline. The anti-tyrosine hydroxylase (TH) antibody was purchased from Chemicon (Temecula, CA). A Histofine mouse stain kit was purchased from Nichirei Biosciences, Inc. (Tokyo, Japan). All of the other reagents were of the highest purity commercially available. Ultrapure water was used in all experiments (Millipore Co.; Billerica, MA).

Animals

Male C57Bl/6 mice weighing 21–25 g were purchased from Charles River Japan. All animals were maintained in a temperature- and humidity-controlled room with free access to a standard diet (MF; Oriental Yeast Co., Ltd., Tokyo, Japan) and tap water.

All the procedures and animal care were approved by the Animal Care and Use Committee, Kyushu University, and carried out in accordance with the Guidelines for Animal Experiments, Kyushu University.

In vivo *Microdialysis*

Animals were anaesthetized with pentobarbital (50 mg/kg, i.p.) and mounted in a stereotaxic frame equipped with a mouse adapter. A guide cannula was implanted into the striatum (co-ordinates from bregma: anterior-posterior: +0.5, lateral-medial: ±2.0, doral-ventral: −2.5 from the skull), as described previously [16]. The guide cannula was fixed to the skull with one stainless steel screw and methylacrylic cement. Four days after implantation, microdialysis experiments were performed under anaesthesia with 2.0% isoflurane. Artificial Ringer's solution (147 mmol/L Na^+, 4 mmol/L K^+, 1.26 mmol/L Ca^{2+}, 1 mmol/L Mg^{2+} and 155.6 mmol/L Cl^{2-}) was pumped through the dialysis probe at a constant flow rate of 2 μL/min.

We collected the dialysate sample for each 20 min time point. The total amount of collected sample was 40 μL. The microdialysis session started after a 120-min equilibration period and the perfusate was changed as described below. Fractions 1–4 were collected while Ringer's solution was perfused, as the baseline. After fraction 4, tyramine (0, 10 or 100 mmol/L) was added to the perfusion fluid. After fraction 8, the perfusion fluid was changed back to Ringer's solution and dialysis was continued through fraction 18. HPLC analysis and ESR measurements were performed using 20 μL of each dialysate sample. The remaining 20 μL was used to measure the H2O2 concentration.

For some experiments, an MAO-A/B inhibitor, either pargyline (30 mg/kg) or tranylcypromine (15 mg/kg), was injected 1 h before the start of baseline recording, to obtain the complete inhibition of MAO-A/B. In other experiments, TH inhibitor alpha-methyl-*p*-tyrosine (250 mg/kg) was injected 4 h before recording, as described previously [17].

Chromatographic conditions

Dopamine and its metabolites were assayed by HPLC coupled with electrochemical detection (ECD). A 20-μL sample was separated on a C18 reverse phase column (MCM column 150 × 4.6 mm, MC Medical, Inc., Tokyo Japan) and detected with an ECD system, which consisted of an ESA Coulochem III (Chelmsford, MA) controller fitted with a guard cell (M5020) and analytical cell set (M5011). The guard cell was set at +450 mV, electrode 1 at 50 mV and electrode 2 at 400 mV. The mobile phase was phosphate buffer containing heptansulphonic acid and the rate of the mobile phase flow through the system was 0.8 mL/min.

Hydroxy-TEMPO and its reaction products were assayed by HPLC coupled with ECD, as described in our previous report [15]. Separation was achieved with a C18 reverse-phase column (MCM column 150 × 4.6 mm, MC Medical Inc., Tokyo Japan). The mobile phase contained 10 mmol/L lithium perchlorate with 30% (v/v) methanol and the HPLC flow rate was 0.5 mL/min. The guard cell was set at +850 mV, electrode 1 at 200 mV and electrode 2 at 800 mV. The reduced form of hydroxy-TEMPO, 4-hydroxy-2,2,6,6,-tetramethyl-N-hydroxypiperidine, was prepared by reduction as described [18].

Hydrogen peroxide concentration assay

The concentration of H_2O_2 in the dialysate was determined by the method of Keston and Brandt [19]. In brief, the oxidation of 2,7-dichlorofluorescin to the fluorescent 2,7-dichlorofluorescein by H_2O_2 was investigated by fluorescence at an excitation wavelength of 510 nm and an emission wavelength of 550 nm with a spectrofluorometer (Tecan, Australia). To discriminate H_2O_2 from other oxidants in the dialysate, another 5 μL of dialysate was reacted with catalase at room temperature for 10 min. The fluorescence intensity was corrected by subtracting the value of the catalase-treated dialysate from that of the untreated dialysate. The concentration of H_2O_2 in the dialysate was obtained from a standard curve (0–10 μmol/L).

Detection of free-radical reactions by X-band ESR

X-band ESR spectra were recorded at room temperature using a JEOL JES-1X ESR spectrometer (microwave power: 5 mW; amplitude of 100-kHz field modulation: 0.06 mT; time constant: 0.03 s; sweep rate: 1 min/10 mT). For the X-band ESR measurements, hydroxy-TEMPO (5 μmol/L) or carboxy-TEMPO (5 μmol/L) was added to the perfusion fluid. The dialysate was mixed with 40 μmol/L potassium ferricyanide to determine the amount of reduced nitroxyl radical. Deferoxamine (200 μmol/L) and DMTU (1 mmol/L) were added to the perfusion fluid with hydroxy-TEMPO to confirm the relationship between the signal reduction of the nitroxyl probe and ROS generation. The ESR spectra were analysed with an ESR Data Analyser (JEOL Co. Ltd., Akishima, Japan). The level of spin probe was determined from the ESR signal intensity by calibrating the signal intensity with that of Mn^{2+}, which was used as the standard.

Immunohistochemistry

TH immunoreactivity was determined as described previously [4,20]. Mice were anaesthetized with sodium pentobarbital (50 mg/kg, i.p.) 5 days after the tyramine perfusion and the brains were perfusion-fixed with 4% paraformaldehyde in 0.1 M phosphate buffer (pH 7.4). Brain sections were embedded in paraffin and paraffin sections (5-μm thick) of the striatum were used for immunohistochemistry. The sections were incubated with anti-tyrosine hydroxylase antibody (1:200) and a Histofine mouse stain kit (Nichirei Biosciences Inc.) was used to detect the primary antibody. The negative control was treated as described above, except that the anti-TH antibody was omitted. After a final wash, the reactivity was visualized with diaminobenzidene (DAB; Nichirei). Counterstaining was then performed with Mayer's haematoxylin.

To examine the association between TH immunoreactivity and the amount of dopamine and its metabolites in the striatum, the brain tissues were homogenized with 10% perchloric acid. After centrifugation at 14 000 g for 15 min, the supernatant was filtered (0.45-μm filter, Minisart RC4; Sartorius Stedim Biotec GmbH, Goettingen, Germany) and analysed for dopamine and its methabolites by HPLC/ECD, as described above.

Rotational behaviour tests

In the animal model of Parkinson's disease, rats receive a unilateral intracerebral injection of 6-hydroxydopamine that causes ipsilateral destruction of dopamine-containing neurons [21]. Because of chronic hemidepletion of dopamine, rats will rotate contralateral to the lesion following injections of dopamine agonists such as levodopa and they rotate in the ipsilateral direction in response to the indirect dopamine agonist amphetamine [22]. Therefore, in this study, mice were tested for rotational behaviour induced by methamphetamine (2.5 mg/kg, i.p.) 5 days after tyramine perfusion with or without hydroxy-TEMPO (5 μM) [10]. The rotations were counted for 40 min. The methamphetamine-induced rotational asymmetry scores were expressed as the ratio of rightward full turns to leftward full turns.

Statistical analysis

Data are expressed as the mean ± SEM. Statistical significance was analysed using either an unpaired Student's *t*-test or Dunnett's test. A probability value of 0.05 was set as the minimum level of statistical significance.

Results

Level of monoamines in the dialysate during intrastriatal tyramine application

The basal level of dopamine was 1.72 ± 0.57 (ng/mL) in the striatal dialysate. The intrastriatal tyramine induced a dose-dependent increase in dopamine levels (Figure 1A), which was suppressed by the dopamine synthesis inhibitor, alpha-methyl-*p*-tyrosine. However, pre-treatment with MAO inhibitors, pargyline or tranylcypromine did not have an influence on this response (Figure 1B). The dopamine metabolites in the dialysate were also increased by the application of tyramine (Table I). The enhanced DOPAC and HVA production was suppressed by pre-treatment with the MAO inhibitors (Table I), because MAO catalyses the oxidation of dopamine to DOPAC and of 3-MT to HVA.

Tyramine is reported to be a good substrate for both MAO A and B (MAO-A/B) and to undergo rapid turnover owing to its metabolism by MAO [23]. However, we could not detect p-hydroxyphenylacetic acid, a metabolite of tyramine, in this study (data not shown).

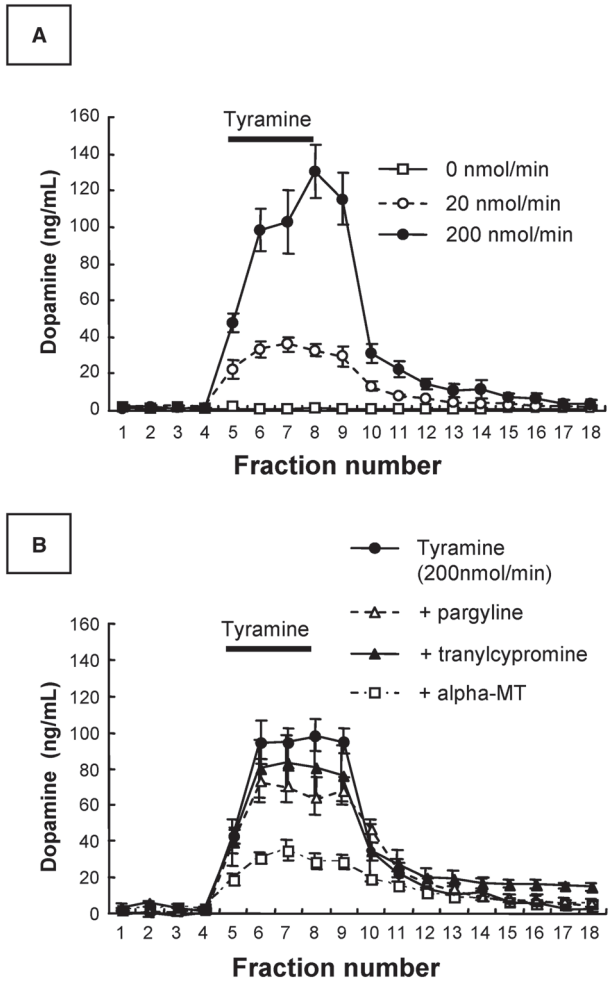

Figure 1. Effect of intrastriatal tyramine on the extracellular level of dopamine (A) and the effect of enzyme inhibitors on the tyramine-induced dopamine elevation (B). The MAO-A/B inhibitors pargyline (30 mg/kg) or tranylcypromine (15 mg/kg) was injected 1 h before the onset of baseline recording. The TH inhibitor alpha-methyl-*p*-tyrosine (alpha-MT, 250 mg/kg) was injected 4 h before baseline recording. Each value represents the mean ± SEM of six animals.

Production of H_2O_2 during intrastriatal tyramine application

The processes by which H2O2 is produced through the oxidation of both dopamine and 3-MT by MAO are presented schematically in Figure 2A. As shown

Table I. Total concentration of dopamine metabolites (ng/mL) during Tyramine perfusion.

Tyramine	0 nmol/min	200 nmol/min		
MAO inhibitor	—	—	pargyline	tranylcypromine
DOPAC	27.9 ± 8.1	61.0 ± 14.2*	0.6 ± 0.3###	0.1 ± 0.1###
3-MT	0.2 ± 0.1	108.3 ± 30.2**	67.0 ± 17.2	94.9 ±19.2
HVA	71.3 ± 11.5	207.1 ± 59.1*	4.2 ± 2.3###	2.9 ± 2.3###

Each value represents the mean ± SEM. *$p < 0.05$ and **$p < 0.01$ vs the no-tyramine (0 nmol/min) group; and ###$p < 0.005$ vs the no-inhibitor tyramine (200 nmol/min) group. Each condition used six animals.

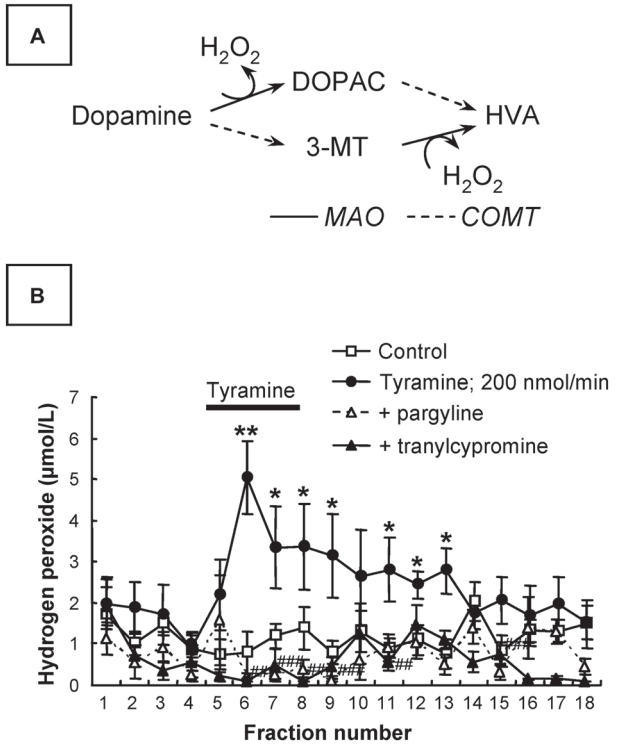

Figure 2. Schematic representation of H_2O_2 generation during dopamine metabolism via MAO (A) and the effect of the intrastriatal tyramine on the extracellular level of H_2O_2 (B). The MAO-A/B inhibitors pargyline (30 mg/kg) or tranylcypromine (15 mg/kg) was injected 1 h before baseline recording began. Each value represents the mean ± SEM. $^{*}p < 0.05$ and $^{**}p < 0.01$ vs the no-tyramine group; and $^{\#\#}p < 0.01$ and $^{\#\#\#}p < 0.005$ vs the no-inhibitor tyramine (200 nmol/min) group. Each condition used six animals.

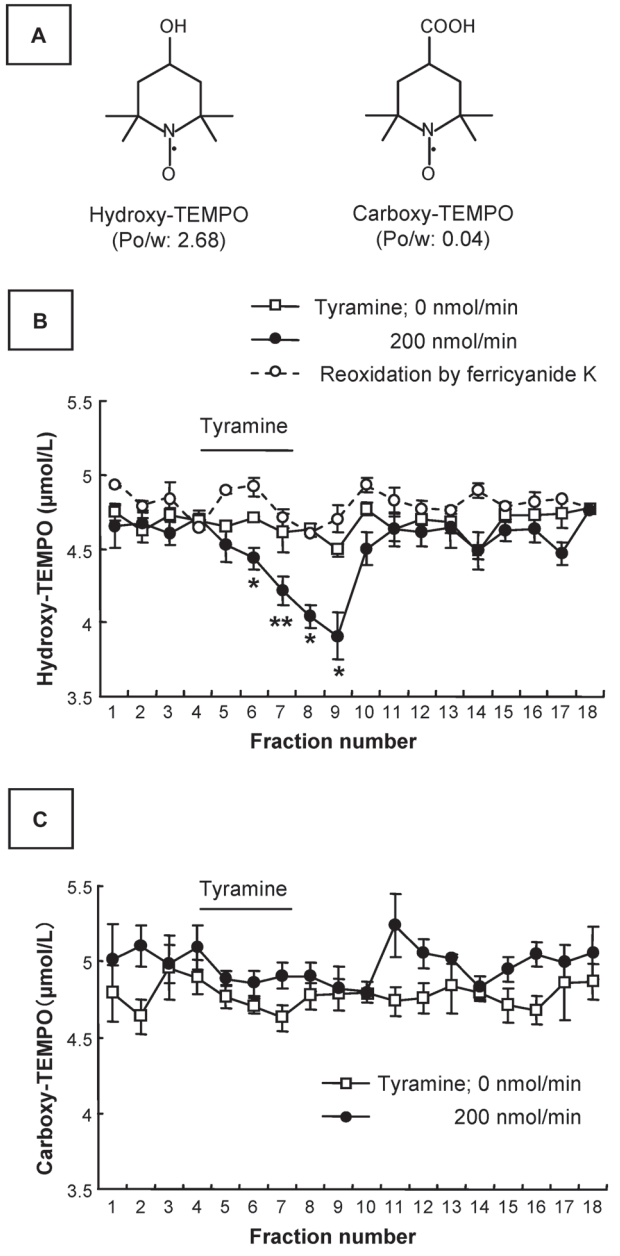

Figure 3. Structure of spin probes (A) and signal decay of hydroxy-TEMPO (B) and carboxy-TEMPO (C) during tyramine application. X-band ESR was performed as described in the Materials and methods section. Each value represents the mean ± SEM.; $^{*}p < 0.05$ and $^{**}p < 0.01$ vs the no-tyramine (0 nmol/min) group. Each condition used five animals.

in Figure 2B, the intrastriatal tyramine application produced a significant increase in the H_2O_2 level. The increase in H_2O_2 was observed during tyramine perfusion and it remained elevated until 100 min after the end of the tyramine perfusion. The possible reason why H_2O_2 levels remains high even after the tyramine perfusion might be related to the relative stability of H_2O_2. Pre-treatment with MAO inhibitors, pargyline or tranylcypromine suppressed the H_2O_2 increase induced by the intrastriatal tyramine. Thus, the oxidation of dopamine and 3-MT by MAO produced H_2O_2 in the striatum of tyramine-treated mice.

Detection of free-radical reactions by X-band ESR. Site-specific spin probes have been used to detect the localized generation of ROS in vivo [11]. Therefore, we measured the ESR signal decay of carboxy- and hydroxy-TEMPO in the dialysate. The structure of spin probes is shown in Figure 3A. The changes of signals from both the spin probes were slightly lower in dialysate obtained from sham-operated mice (Figures 3B and C, open squares). The ESR signal of hydroxy-TEMPO, which is membrane permeable, was decreased for 80 min after the start of tyramine perfusion (Figure 3B, closed circles). This decrease was recovered by the addition of potassium ferricyanide (Figure 3B, open circles), indicating that hydroxy-TEMPO was reduced in the presence of tyramine to its corresponding hydroxylamine. The ESR signal of carboxy-TEMPO, which is not membrane permeable, was not affected by the tyramine application (Figure 3C, indicated by closed circles).

We recently reported that the hydroxylamine form was generated as a reaction product of hydroxy- TEMPO with ROS, using HPLC-ECD

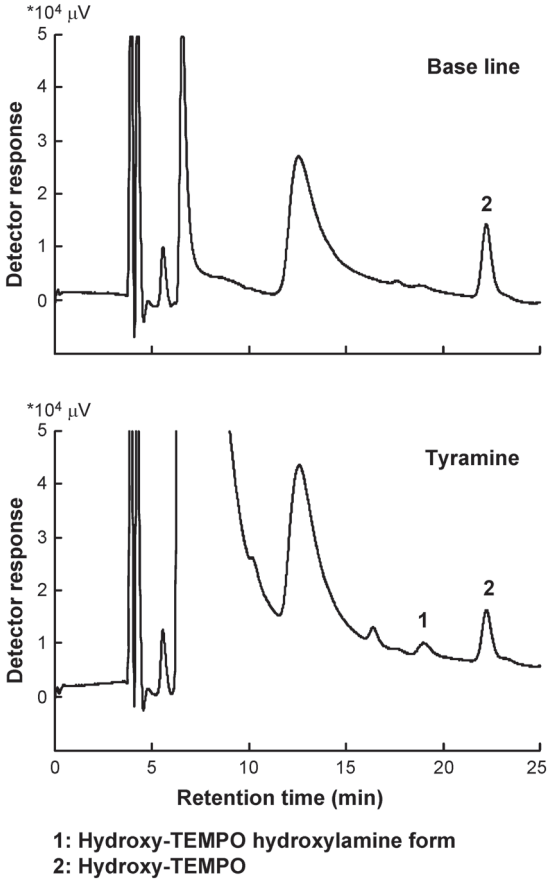

Figure 4. HPLC/ECD chromatogram of hydroxy-TEMPO and its corresponding hydroxylamine during dopamine metabolism. Samples obtained from baseline and tyramine fractions were subjected to HPLC analysis. The experimental conditions are described in the Materials and methods section.

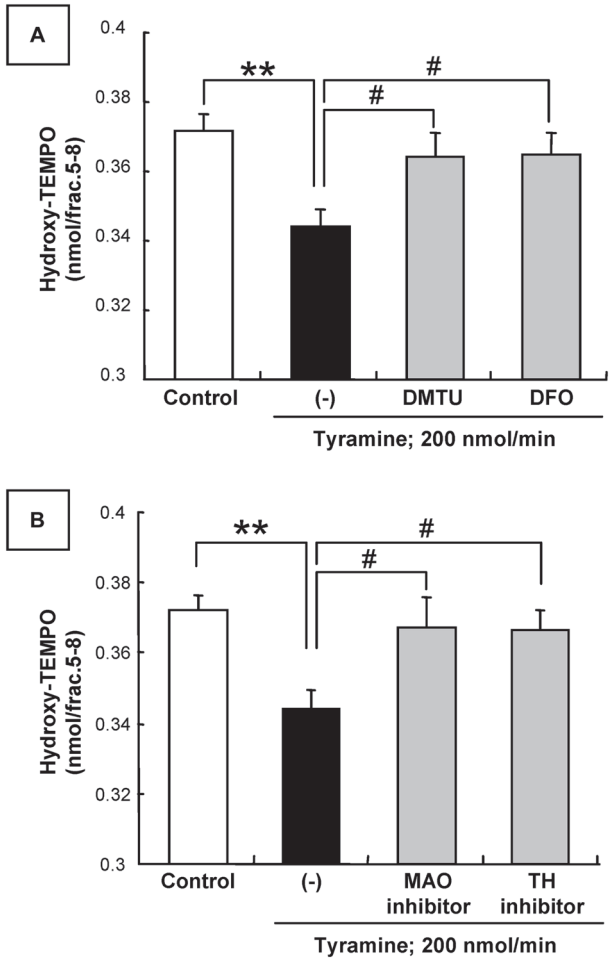

Figure 5. Effect of antioxidant or enzymatic inhibitors on the hydroxy-TEMPO ESR signal during tyramine application. Deferoxamine (200 μmol/L) or DMTU (1 mmol/L) was added to the perfusion fluid with hydroxy-TEMPO (A). In (B), the MAO-A/B inhibitor pargyline (30 mg/kg) or TH inhibitor alpha-methyl-*p*-tyrosine (250 mg/kg) was injected, respectively, 1 h and 4 h before the start of baseline recording. X-band ESR was performed as described in the Materials and methods section. Each value represents the mean ± SEM. $^{**}p < 0.01$ vs the no-tyramine group; and $^{\#}p < 0.05$ vs the no-inhibitor tyramine (200 nmol/min) group. Each condition used four animals.

[15]. Therefore, we analysed the reaction products of hydroxy-TEMPO in the dialysate during the intrastriatal tyramine application. Figure 4 shows a typical HPLC chromatogram of the dialysate obtained from a base-line fraction and from a fraction taken during the intrastriatal tyramine application. The peaks of hydroxy-TEMPO hydroxylamine and hydroxy-TEMPO appeared at 19.0 and 22.2 min, respectively. The concentration of these products estimated from chromatograms showed that the level of hydroxylamine form generation was in agreement with the decrease of hydroxy-TEMPO (hydroxy-TEMPO: 4.36 μM, hydroxylamine form: 0.34 μM in base line and hydroxy-TEMPO: 3.17 μM, hydroxylamine form: 1.52 μM in tyramine perfusion). In the chromatogram of the fraction taken during the tyramine application, the peaks of tyramine, dopamine and its metabolites appeared within 11 min and at 16.4 min. This result directly verifies the conversion of the nitroxyl radical to the corresponding hydroxylamine form during tyramine perfusion. A peak at 12.6 min caused by measurement noise was always observed.

To confirm that hydroxy-TEMPO was reduced by the ROS generated during dopamine metabolism by MAO, the ESR measurements of signal decay were performed with MAO-inhibitor pre-treatment or in the presence of antioxidants. Figure 5A shows that the simultaneous perfusion of DMTU (an •OH scavenger) or deferoxamine (an iron-chelating agent) significantly suppressed the signal decay of hydroxy-TEMPO (Figure 5B). Furthermore, the decay of the ESR signal was also suppressed by pre-treatment with pargyline or alpha-methyl-*p*-tyrosine. These results indicate that the decrease of ESR signal reflected the reduction of the hydroxy-TEMPO by ROS generated during dopamine metabolism by MAO.

The spin trapping technique is a suitable way to detect the •OH radical. In our preliminary experiments, we tried to identify ROS using spin trapping, but we could not detect the target signal using any of

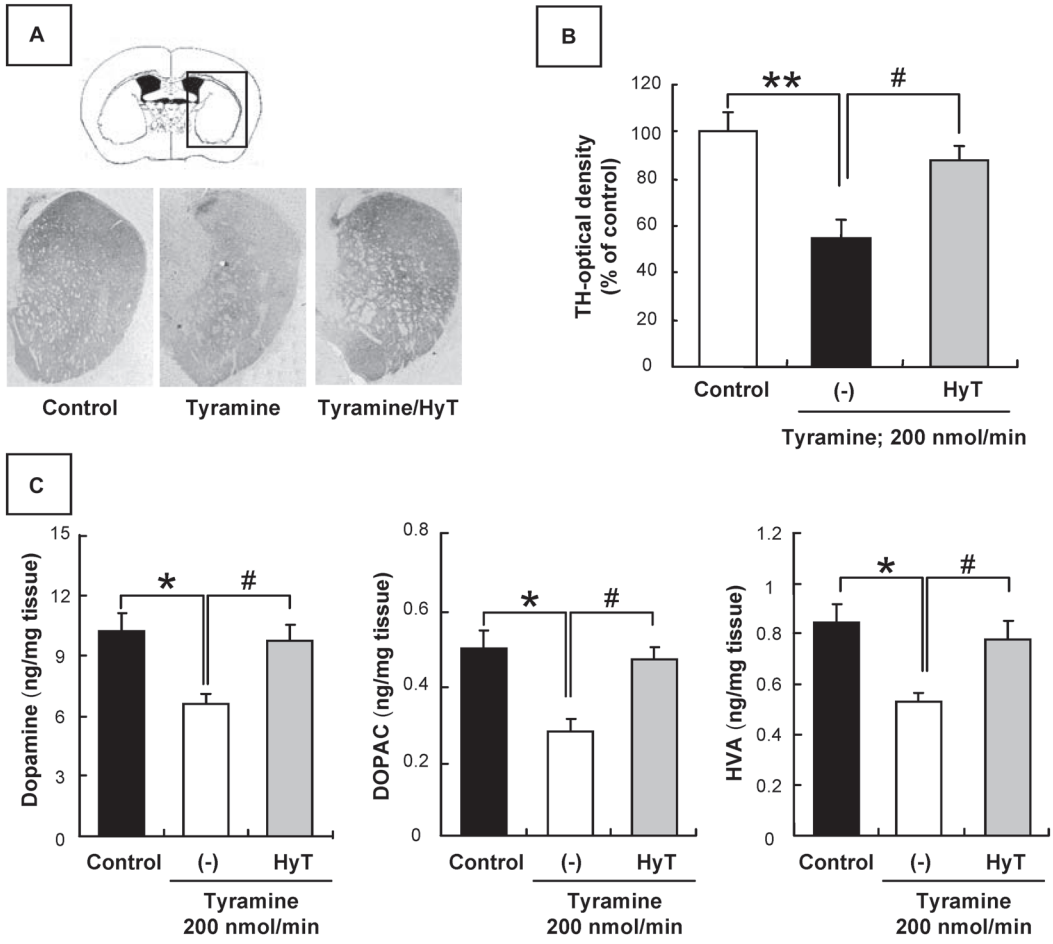

Figure 6. Effect of hydroxy-TEMPO on tyramine-induced neurotoxicity in the striatum 5 days after tyramine application. Coronal sections of the striatum were stained with an anti-TH antibody (A) and the relative TH-immunoreactivity (B) and amounts of dopamine and its metabolites (C) were determined. Each value represents the mean ± SEM. $^{*}p < 0.05$ and $^{**}p < 0.01$ vs the no-tyramine group; and $^{\#}p < 0.05$ vs the tyramine (200 nmol/min) without hydroxy-TEMPO (HyT) group. Each condition used five animals in (B) and six animals in (C).

the commercial available spin-trap agents because of their lack of permeability or the high background noise due to the tyramine (data not shown). Asmus and Nigam [13] reported that hydroxy-TEMPO reacted with •OH radical ($k = 3.4^{*}10^{9}$) or other radicals. Therefore, in this study, we used hydroxy-TEMPO as spin probe to detect the free radical reaction in the brain of living mice.

Tyrosine hydroxylase immunostaining in the striatum

Representative photographs of TH immunostaining in the striatum are shown in Figure 6A. A decrease in the density of TH-immunopositive fibres was observed 5 days after tyramine administration and level of immunoreactivity against striatal TH decreased to 55% of the control (Figure 6B). Consequently, the levels of dopamine and its metabolites in the striatum of tyramine-perfused mice were significantly decreased compared with their levels in control mice (Figure 6C). These findings suggest that the ROS generation, which was monitored with hydroxy-TEMPO during dopamine metabolism, caused a decrease in the density of TH-immunopositive fibres in the striatum. Intriguingly, hydroxy-TEMPO obviously improved both the tyramine-induced decrease in TH immunoactivity and the dopamine concentration.

Effects of hydroxy-TEMPO on tyramine-induced central dopaminergic dysfunction

To assess the neuroprotective effect of hydroxy-TEMPO on dopamine-regulated motor function, the methamphetamine-induced rotational response in mice was examined 5 days after tyramine perfusion with hydroxy-TEMPO. Methamphetamine treatment markedly evoked a robust ipsilateral rotational response in the tyramine-perfused mice (Figure 7), suggesting that the abnormal behaviour of the tyramine-perfused mice was related to the striatal dopamine content. Notably, the simultaneous perfusion of hydroxy-TEMPO dramatically improved the neurological effect.

Discussion

Our microdialysis experiments combined with X-band ESR/*in vivo* spin probe techniques indicated that

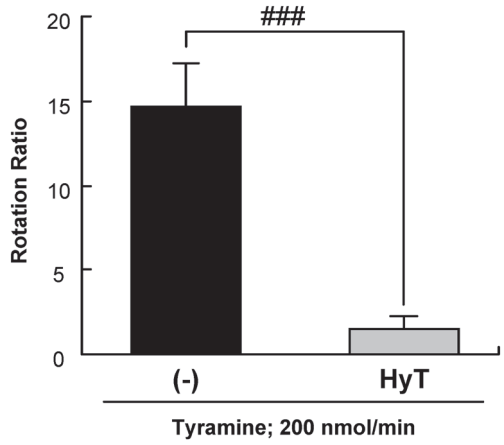

Figure 7. Effect of hydroxy-TEMPO on a tyramine-induced behavioural abnormality. Mice were tested for methamphetamine-induced rotational behaviour 5 days after tyramine application. The rotations were counted for 40 min and expressed the ratio of rightward full turns to leftward full turns. Each value represents the mean ± SEM. $^{###}p < 0.005$ vs the tyramine (200 nmol/min) without hydroxy-TEMPO (HyT) group. Each condition used six animals.

tyramine application in the striatum caused the generation of ROS during dopamine metabolism. The appearance of ROS was associated with a decrease in the density of TH-immunopositive fibres in the striatum, resulting in a decrease in dopamine and the appearance of abnormal neurological symptoms. These outcomes were related to the degeneration of dopaminergic neurons and were improved by the simultaneous perfusion of hydroxy-TEMPO. Our results not only confirm that ROS are generated during dopamine metabolism, but also demonstrate their association with the progressive degeneration of dopaminergic neurons.

Because only a small fraction of the dopamine in cells is oxidatively metabolized and assumed to be toxic, we used the tyramine application model to induce excess dopamine metabolism. Schmidt and Ferger [16] reported that •OH is generated during tyramine application, by estimating its level using the salicylate assay. This assay is highly sensitive for analysing •OH production; however, it does not accurately indicate where the •OH is generated. The salicylate assay reflects the reaction not only in the brain, but also in the microdialysis probe or cannula. To solve this problem, we used two site-specific spin probes, hydroxy-TEMPO and carboxy-TEMPO, that have different membrane permeabilities. We used the conversion of the nitroxyl radical to its corresponding hydroxylamine form as an index to detect the ROS generation during dopamine metabolism. The ESR signal of hydroxy-TEMPO was decreased in the dialysate collected from tyramine-perfused mice (Figure 3). However, nitroxyl radicals can also be converted to their hydroxylamine form by reacting with ascorbate [18] or superoxide anion radicals [14]. To identify ROS, DMTU or deferoxiamine was added to the perfusion fluid with the hydroxy-TEMPO. The decrease in the hydroxy-TEMPO ESR signal was suppressed by these antioxidants, as well as by pre-treatment with TH or MAO inhibitors (Figure 5). These results suggest that the ROS such as •OH might be generated in cells through metal-catalysed redox reactions (Fenton reactions) during dopamine metabolism.

Decreases in dopamine and its metabolites in the striatal nuclei in the brain are associated with the progressive degeneration of dopaminergic neurons, such as in Parkinson's disease [24,25]. TH activity itself is markedly decreased in the substantia nigra and striatum in the Parkinson's disease brain [26], which is one of the mechanisms for the decrease in dopamine. Borges et al. [27] reported that TH is modified by S-glutathionylation in the presence of a sulphydryl oxidant and that this post-translational modification results in a decrease in TH catalytic function. Moreover, S-Glutathionylation has been suggested to be accelerated by ROS [28]. In fact, it was reported that antioxidants exert a protective effect on TH immunoreactivity [29]. In this study, we demonstrated that decreases in TH immunostaining and the dopamine content were induced by tyramine, resulting in abnormal neurological symptoms (Figures 6 and 7). Hydroxy-TEMPO, the spin probe used to detect ROS, could suppress these defects, probably by acting as an antioxidant.

Mitochondrial complex I dysfunction is also believed to be associated with the pathophysiology of Parkinson's disease [30,31]. Classical dopaminergic degenerative animal models use neuron-specific neurotoxins such as 6-hydroxydopamine [32,33], MPTP/MPP^+ [34] or rotenone [35], which act in part via oxidative stress to induce mitochondrial complex I dysfunction. In addition, several other pathogenic mechanisms contribute to the oxidative stress that causes the degeneration of dopaminergic neurons [36]. These mechanisms, including the metabolism of dopamine via MAO, may be mutually related and exacerbate the oxidative stress leading to dopaminergic neuron degeneration.

Ultimately, our results indicate that ROS generation during dopamine metabolism may induce the dopamine-related insult. ROS such as •OH consequently represent a promising molecular target for therapeutic interventions designed to slow the progression of dopaminergic neuron degeneration.

Declaration of interest: Financial support for this work was provided by the Japan Science and Technology Agency. The authors report no conflicts of interest. The authors alone are responsible for the content and writing of the paper.

References

[1] Pedrosa R, Soares-da-Silva P. Oxidative and non-oxidative mechanisms of neuronal cell death and apoptosis by L-3,

4-dihydroxyphenylalanine (L-DOPA) and dopamine. Br J Pharmacol 2002;137:1305–1313.
[2] Ziv I, Melamed E, Nardi N, Luria D, Achiron A, Offen D, Barzilai A. Dopamine induces apoptosis-like cell death in cultured chick sympathetic neurons—a possible novel pathogenetic mechanism in Parkinson's disease. Neurosci Lett 1994;170:136–140.
[3] Jones SR, Gainetdinov RR, Jaber M, Giros B, Wightman RM, Caron MG. Profound neuronal plasticity in response to inactivation of the dopamine transporter. Proc Natl Acad Sci USA 1998;95:4029–4034.
[4] Hastings TG, Lewis DA, Zigmond MJ. Role of oxidation in the neurotoxic effects of intrastriatal dopamine injections. Proc Natl Acad Sci USA 1996;93:1956–1961.
[5] Chen L, Ding Y, Cagniard B, Van Laar AD, Mortimer A, Chi W, Hastings TG, Kang UJ, Zhuang X. Unregulated cytosolic dopamine causes neurodegeneration associated with oxidative stress in mice. J Neurosci 2008;28:425–433.
[6] Cohen G, Farooqui R, Kesler N. Parkinson disease: a new link between monoamine oxidase and mitochondrial electron flow. Proc Natl Acad Sci USA 1997;94:4890–4894.
[7] Mallajosyula JK, Kaur D, Chinta SJ, Rajagopalan S, Rane A, Nicholls DG, Di Monte DA, Macarthur H, Andersen JK. MAO-B elevation in mouse brain astrocytes results in Parkinson's pathology. PLoS ONE 2008;3:e1616.
[8] Rogoza RM, Fairfax DF, Henry P, N-Marandi S, Khan RF, Gupta SK, Mishra RK. Electron spin resonance spectroscopy reveals alpha-phenyl-N-tert-butylnitrone spin-traps free radicals in rat striatum and prevents haloperidol-induced vacuous chewing movements in the rat model of human tardive dyskinesia. Synapse 2004;54:156–163.
[9] Anzai K, Aikawa T, Furukawa Y, Matsushima Y, Urano S, Ozawa T. ESR measurement of rapid penetration of DMPO and DEPMPO spin traps through lipid bilayer membranes. Arch Biochem Biophys 2003;415:251–256.
[10] Liang Q, Smith AD, Pan S, Tyurin VA, Kagan VE, Hastings TG, Schor NF. Neuroprotective effects of TEMPOL in central and peripheral nervous system models of Parkinson's disease. Biochem Pharmacol 2005;70:1371–1381.
[11] Yamato M, Egashira K, Utsumi H. Application of *in vivo* ESR spectroscopy to measurement of cerebrovascular ROS generation in stroke. Free Radic Biol Med 2003;35: 1619–1631.
[12] Willson RL. Reaction of triacetoneamine-N-oxyl with hydroxyl radicals. Int J Radiat Biol Relat Stud Phys Chem Med 1972;21:401–403.
[13] Asmus KD, Nigam S. Kinetics of nitroxyl radical reactions. A pulse-radiolysis conductivity study. Int J Radiat Biol Relat Stud Phys Chem Med 1976;29:211–219.
[14] Krishna MC, Grahame DA, Samuni A, Mitchell JB, Russo A. Oxoammonium cation intermediate in the nitroxide-catalyzed dismutation of superoxide. Proc Natl Acad Sci USA 1992; 89:5537–5541.
[15] Kudo W, Yamato M, Yamada K, Kinoshita Y, Shiba T, Watanabe T, Utsumi H. Formation of TEMPOL-hydroxylamine during reaction between TEMPOL and hydroxyl radical: HPLC/ECD study. Free Radic Res 2008;42:505–512.
[16] Schmidt N, Ferger B. The biogenic trace amine tyramine induces a pronounced hydroxyl radical production via a monoamine oxidase dependent mechanism: an *in vivo* microdialysis study in mouse striatum. Brain Res 2004;1012:101–107.
[17] Watanabe S, Fusa K, Takada K, Aono Y, Saigusa T, Koshikawa N, Cools AR. Effects of alpha-methyl-p-tyrosine on extracellular dopamine levels in the nucleus accumbens and the dorsal striatum of freely moving rats. J Oral Sci 2005; 47:185–190.

This paper was first published online on Early Online on 16 December 2009.

[18] Bobko AA, Kirilyuk IA, Grigor'ev IA, Zweier JL, Khramtsov VV. Reversible reduction of nitroxides to hydroxylamines: roles for ascorbate and glutathione. Free Radic Biol Med 2007; 42:404–412.
[19] Keston AS, Brandt R. The fliorometric analysis of ultramicro quantites of hydrogen peroxide. Anal Biochem 1965;11:1–5.
[20] Milusheva E, Baranyi M, Kittel A, Sperlagh B, Vizi ES. Increased sensitivity of striatal dopamine release to H2O2 upon chronic rotenone treatment. Free Radic Biol Med 2005; 39:133–142.
[21] Ungerstedt U, Arbuthnott GW. Quantitative recording of rotational behavior in rats after 6-hydroxy-dopamine lesions of the nigrostriatal dopamine system. Brain Res 1970;24:485–493.
[22] Ungerstedt U. Striatal dopamine release after amphetamine or nerve degeneration revealed by rotational behaviour. Acta Physiol Scand Suppl 1971;367:49–68.
[23] Juorio AV, Boulton AA. The effect of some precursor amino acids and enzyme inhibitors on the mouse striatal concentration of tyramines and homovanillic acid. J Neurochem 1982;39:859–863.
[24] Bernheimer H, Hornykiewicz O. Decreased homovanillic acid concentration in the brain in Parkinsonian subjects as an expression of a disorder of central dopamine metabolism. Klin Wochenschr 1965;43:711–715.
[25] Ehringer H, Hornykiewicz O. Distribution of noradrenaline and dopamine (3-hydroxytyramine) in the human brain and their behavior in diseases of the extrapyramidal system. Klin Wochenschr 1960;38:1236–1239.
[26] Nagatsu T, Kato T, Numata Y, Ikuta K, Sano M. Phenylethanolamine N-methyltransferase and other enzymes of catecholamine metabolism in human brain. Clin Chim Acta 1977;75:221–232.
[27] Borges CR, Geddes T, Watson JT, Kuhn DM. Dopamine biosynthesis is regulated by S-glutathionylation. Potential mechanism of tyrosine hydroxylast inhibition during oxidative stress. J Biol Chem 2002;277:48295–48302.
[28] Giustarini D, Rossi R, Milzani A, Colombo R, Dalle-Donne I. S-glutathionylation: from redox regulation of protein functions to human diseases. J Cell Mol Med 2004;8: 201–212.
[29] Oyagi A, Oida Y, Hara H, Izuta H, Shimazawa M, Matsunaga N, Adachi T, Hara H. Protective effects of SUN N8075, a novel agent with antioxidant properties, in *in vitro* and *in vivo* models of Parkinson's disease. Brain Res 2008;1214:169–176.
[30] Dawson TM, Dawson VL. Molecular pathways of neurodegeneration in Parkinson's disease. Science 2003;302: 819–822.
[31] Schapira AH, Cooper JM, Dexter D, Jenner P, Clark JB, Marsden CD. Mitochondrial complex I deficiency in Parkinson's disease. Lancet 1989;1:1269.
[32] Glinka Y, Tipton KF, Youdim MB. Nature of inhibition of mitochondrial respiratory complex I by 6-Hydroxydopamine. J Neurochem 1996;66:2004–2010.
[33] Glinka YY, Youdim MB. Inhibition of mitochondrial complexes I and IV by 6-hydroxydopamine. Eur J Pharmacol 1995;292:329–332.
[34] Nicklas WJ, Vyas I, Heikkila RE. Inhibition of NADH-linked oxidation in brain mitochondria by 1-methyl-4-phenylpyridine, a metabolite of the neurotoxin, 1-methyl-4-phenyl-1,2,5,6-tetrahydropyridine. Life Sci 1985;36:2503–2508.
[35] Saravanan KS, Sindhu KM, Mohanakumar KP. Acute intranigral infusion of rotenone in rats causes progressive biochemical lesions in the striatum similar to Parkinson's disease. Brain Res 2005;1049:147–155.
[36] Tsang AH, Chung KK. Oxidative and nitrosative stress in Parkinson's disease. Biochim Biophys Acta 2009;1792: 643–650.